Separation Science and Technology
Publication details, including instructions for authors and subscription information:
http://www.informaworld.com/smpp/title~content=t713708471

Treatment of Liming Effluent from Tannery using Membrane Separation Processes

Chandan Das[a]; Sirshendu De[a]; Sunando DasGupta[a]
[a] Department of Chemical Engineering, Indian Institute of Technology, Kharagpur, India

To cite this Article Das, Chandan , De, Sirshendu and DasGupta, Sunando(2007) 'Treatment of Liming Effluent from Tannery using Membrane Separation Processes', Separation Science and Technology, 42: 3, 517 — 539
To link to this Article: DOI: 10.1080/01496390601120680
URL: http://dx.doi.org/10.1080/01496390601120680

Separation Science and Technology, 42: 517–539, 2007

ISSN 0149-6395 print/1520-5754 online
DOI: 10.1080/01496390601120680

Treatment of Liming Effluent from Tannery using Membrane Separation Processes

Chandan Das, Sirshendu De, and Sunando DasGupta
Department of Chemical Engineering, Indian Institute of Technology, Kharagpur, India

Abstract: A treatment method of liming effluent of a tannery is tested using hybrid membrane separation processes. The effluent after gravity settling and alum coagulation is subjected to ultrafiltration followed by nanofiltration. The optimum alum dose is obtained by analyzing the effluent using various concentrations of alum. The membrane separation processes are conducted in a continuous cross flow mode. The effects of operating conditions e.g., transmembrane pressure difference, and cross flow velocity (Reynolds number) on the permeate flux are analyzed. Effects of change in hydrodynamic conditions in various flow regimes, e.g., laminar, laminar with turbulent promoter, and turbulent flow on flux improvement have been studied. A resistance-in-series model for flux decline during the filtration process is proposed. COD, BOD, TDS, TS, pH, Ca^{2+} concentration, Cl^- concentration and conductivity are measured before and after each operation. The potential of the dried sludge as organic fertilizer is also explored.

Keywords: Leather effluent, ultrafiltration, nanofiltration, turbulent promoter, resistance-in-series model

INTRODUCTION

Wastewaters generated from the leather industry are considered one of the most pollutant wastes due to the presence of an appreciable amount of organic materials (mainly dissolved fats, flesh, keratin, bones, etc.) and inorganic chemicals (various salts like sodium chloride, sodium sulfate,

Received 17 August 2006, Accepted 22 October 2006
Address correspondence to Sunando DasGupta, Department of Chemical Engineering, Indian Institute of Technology, Kharagpur 721302, India. Tel.: +91–3222–283922; Fax: +91–3222–255303; E-mail: sunando@che.iitkgp.ernet.in

sodium sulfide, calcium hydroxide, etc). The presence of these substances causes high COD, BOD, TDS, TS, conductivity etc. In the process, a huge amount of organic as well as inorganic chemicals are discharged, causing widespread aqueous and soil pollution.

Nowadays it is common practice to treat the different waste water separately than mixing all the effluents (1). The liming process employs the treatment of soaked hides and skins with milk of lime with or without the addition of sharpening agents like sulphides, cyanides, amines, markaptans etc. The objectives of the liming operation are to remove the hairs, nails, hooves, and other keratinous matters, natural grease and fats, to swell up and to split up the fibers to the desired extent, and to bring the collagen to a proper condition for satisfactory tannage.

A liming unit employs about 15% of the total water consumed in a tannery so recycling is required for reducing the consumption of water (2). Ahmed et al. have worked on the treatment of the liming effluent by nanofiltration (3). They have studied the effect of precipitation followed by nanofiltration to reduce the conductivity, turbidity, and COD of the pollution generated by sulfides in the effluent. Unhairing effluent treatment by an activated sludge system is also reported (4). More than 99% of BOD and around 80% of the COD have been removed by an activated sludge system. Wastewater treatment from various process industries, namely, textile, leather, paint, paper and pulp industries etc. have adopted membrane based separations (5–8). With reduction in membrane cost, the membrane based technologies have found widespread applications in treatment of wastes emerging from various process industries (9, 10). Application possibilities of various membrane separation units, e.g., UF, NF, and RO to treat the effluent from different units of tannery are discussed and presented in the review article of Cassano et al. (11). Soaking effluent from a tannery is treated by a hybrid separation process involving gravity settling, coagulation by alum followed by nanofiltration and reverse osmosis (12). It is reported that COD and BOD of the permeate of RO are well below the discharge limit. The application of NF to the effluent of degreasing (13) is also reported. Use of NF and RO for treatment of chromium rich tanning effluent is widely studied (14). Use of UF to treat the liming effluent is conceptually proposed by Cassano et al. (11).

The objective of the present work is to formulate a scheme to treat the liming effluent using a hybrid process, including gravity settling, alum coagulation, ultrafiltration, and nanofiltration. The optimum alum dose is identified. The fertilizer value of the produced sludge is tested. The supernatant liquor is subjected to cross flow ultrafiltration followed by nanofiltration in a continuous mode of operation. Effects of operating pressure and change in hydrodynamics (laminar, laminar with turbulent promoter, and turbulent flow regime) on the permeate flux are observed. A resistance-in-series model is proposed to quantify the flux decline with a first order kinetic model for the build up of the polarized layer. The treatment performance is finally evaluated in

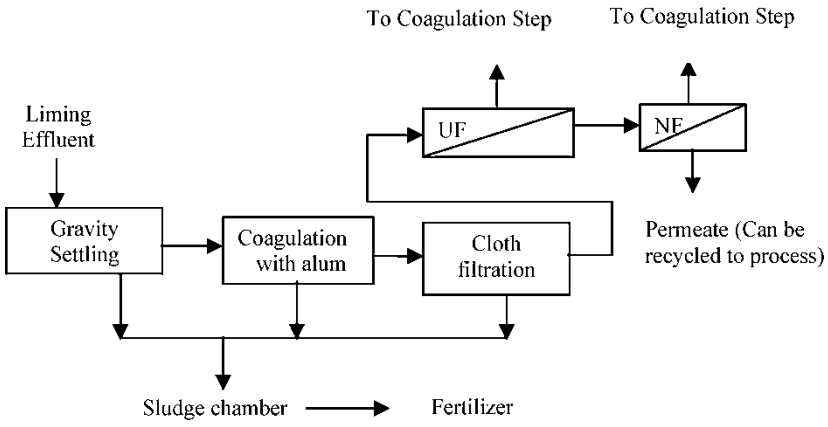

Figure 1. Proposed scheme for the treatment of liming effluent.

terms of various properties like BOD, COD, TS, conductivity, etc. The proposed scheme of the treatment process is presented in Fig. 1.

EXPERIMENTAL

Feed Solution and Materials

The liming bath is obtained from M/s, Alison Tannery, Kolkata. India. Table 1 represents the characterization of the effluent. Commercial alum is used for coagulation. Chemicals required for COD and BOD determination are purchased from Merck Limited, India and Loba Chemie, India and are of analytical grade. All the reagents are used without further treatment.

Thin film composite membranes are used for both UF and NF. The UF membrane is of molecular weight cut off of 5 K with a hydraulic resistance

Table 1. Characterization of effluent

	pH	Conductivity $\times 10^{-1}$ (s/m)	TS (ppm)	TDS (ppm)	COD (ppm)	BOD (ppm)	Cl^- (ppm)	Ca^{++} (ppm)
Feed	13.14	44	60900	29480	15040	5784.6	22980	1400
Feed after gravity settling	12.81	36.5	54600	25500	8800	3384.6	23800	1420
After alum dose	6.8	28.7	47200	19000	3500	1346	21000	1300

of $25.6 \times 10^{12}\ m^{-1}$. The membrane is supplied by Permionics Membranes Pvt. Ltd., Gorwa, Vadodara, India. The NF membrane is 400 MWCO with a hydraulic resistance of $38.5 \times 10^{12}\ m^{-1}$. This membrane is obtained from M/s, Genesis Membrane Sepratech Pvt. Ltd., Mumbai, India.

Optimization of Alum Dose

Nine graduated cylinders of 50 ml capacity with different dosages of alum are used for coagulation study using commercial alum. To get the optimum alum dose, concentrations of 0.05, 0.1, 0.2, 0.3, 0.5, 1, 2, 3, and 5% (weight by volume) are used.

Feed Coagulation

The liming effluent is used after a week of gravity settling. Before alum coagulation, the supernatant is siphoned out. Coagulation experiments are conducted with different dosages of alum for twenty–four hours. It may be noted that beyond half an hour, the rate of coagulation remains almost unchanged. The optimum alum dose is established by examining various properties (e.g., pH, TDS, conductivity, TS, COD, turbidity) of supernatant solutions. The effluent is subjected to coagulation with optimum alum dosing in a 40 l bucket. The sludge is kept under sunlight for drying.

Membrane Cell

For filtration operation, a rectangular cross-flow cell is used. The length and width of the module are 26.1 and 4.9 cm, respectively. The flow channel is formed by placing two silicon rubber gaskets over the membrane in between two matching stainless steel flanges. The height of the flow channel is determined to be 3.4 mm after tightening the two flanges. For experiments with turbulent promoters, sixteen equispaced thin wires of a diameter of 0.19 mm are placed laterally (along the width of the channel) in between the two gaskets. The spacing between the turbulent promoters is 14.0 mm. The same experimental set up is used for UF as well as NF using suitable membranes. The schematic of the experimental setup is available elsewhere (14).

Operating Conditions

Operating conditions are presented in Table 2. In turbulent flow regime, ultrafiltration experiments are conducted at three different operating pressures of

Table 2. Operating conditions for cross flow experiments

Operating condition	Pressure (kPa)	Reynolds number
Ultrafiltration		
Laminar (with and without promoter)	276, 414, 552	680, 1020, 1360
Turbulent	759, 828, 897	4762, 5442, 6122
Nanofiltration		
Laminar (with and without promoter)	828, 966, 1104	680, 1020, 1360
Turbulent	828, 966, 1104	4762, 5442, 6122

759, 828, and 897 kPa. At 759 kPa, experiments are carried out at Reynolds numbers of 4762, 5442, and 6122, whereas at 828 and 897 kPa experiments are conducted at a Reynolds number of 4762 only.

Experimental Procedure for Membrane Separations

A clean membrane is compacted at a pressure higher than its operating pressure for 3 h using distilled water. Membrane permeability is determined using distilled water. Flux values at various operating pressures are measured and the slope of the flux versus the pressure plot gives the permeability. The membrane permeabilities of NF 400 and UF 5 K are $2.6 \times 10^{-11}\,\mathrm{m/Pa \cdot s}$ and $3.914 \times 10^{-11}\,\mathrm{m/Pa \cdot s}$ respectively. The effluent is placed in a stainless steel feed tank of 10 l capacity. A high pressure plunger pump is used to feed the effluent into the cross-flow membrane cell. The retentate stream is recycled to the feed tank routed through a rotameter. The permeate stream is also recycled to maintain a constant concentration in the feed tank. A bypass line from the pump delivery to the feed tank is provided. The two valves in the bypass and the retentate lines are used to vary the pressure and the flow rate through the cell, independently. Cumulative volumes of permeate are collected during the experiment. The values of the permeate flux are determined from the slopes of the cumulative volume versus the time plot. Permeate samples are collected at different times for analysis. The duration of the cross-flow experiment is one hour. Once an experimental run is over, the membrane is thoroughly washed, in situ, with distilled water for thirty minutes applying a maximum pressure of 200 kPa. The cross-flow channel is then dismantled and the membrane is dipped in 0.12 (N) hydrochloric acid solution for three hours. Next, it is washed carefully with distilled water to remove traces of acid. The cross-flow cell is reassembled and the membrane permeability is again measured. It is observed that the membrane permeability remains almost constant between successive runs.

Analysis

Feed and permeate calcium and chloride are estimated by Orion Aplus™ Benchtop Ion Meter (supplied by M/s, Thermo Electron Corporation, Beverly, MA, U.S.A.) using ion specific electrodes. COD and BOD values of each stream are measured by standard techniques (15). The conductivities and TDS of all the streams are measured by an auto ranging conductivity meter (Chemito 130 manufactured by Toshniwal Instruments, India). pH of the samples is measured by a pH meter, supplied by Toshniwal Instruments, India. Total solids (TS) of all the samples are measured by weighing a known volume of sample in a petri dish and keeping it in a vacuum oven maintained at 105 $\pm$ 2°C, till complete drying of the sample. The powdered form of the sludge from coagulation is analyzed for its fertilizer value.

THEORY

Flux Decline Analysis

The permeate flux at any point of time is expressed as,

$$v_w = \frac{\Delta P}{\mu[R_m + R_p(t)]} \tag{1}$$

where, R_m is the membrane hydraulic resistance and R_p is the polarized layer resistance. The polarized layer resistance is a function of time. The time development of the polarized layer resistance is assumed to occur according to a first order kinetics as follows:

$$\frac{dR_p}{dt} \propto (R_p^s - R_p) \tag{2}$$

R_p^s is the steady state polarized layer resistance. Equation (2) can be expressed as,

$$\frac{dR_p}{dt} = k(R_p^s - R_p) \tag{3}$$

where k is the first order rate constant. The above equation can be integrated with the initial condition, $R_p = 0$ at $t = 0$,

$$R_p = R_p^s[1 - \exp(-kt)] \tag{4}$$

Therefore, the constant 'k' is evaluated from the straight line plot of ln (R_p^s/($R_p^s - R_p$) versus time, passing through origin.

RESULTS AND DISCUSSIONS

Pretreatment

Table 1 represents various properties of the supernatant of gravity settled liquor. Various properties of the clear liquid after coagulation at different alum concentrations are presented in Table 3. The table shows that the COD of the clarified liquor decreases with alum concentration and beyond 2%, the change is gradual and TDS, conductivity, and TS concentration increase significantly. It may also be observed that with increase of alum concentration, the turbidity of the solution decreases (with more settling of solids) and beyond 2% the turbidity increases rapidly. The pH of the supernatant is close to normal pH ($\sim$6.8) at 2% alum concentration and it decreases further with increase in alum dose. From these observations, 2% is selected as the optimum concentration of alum for coagulation. The supernatant liquor is then prefiltered through a fine cloth. The dried and pulverized sludge is analyzed for its fertilizer value and compared with vermi compost (Table 4). From Table 4 it is shown that the properties of the sludge are close to those of vermi compost. As a result, the sludge (1.3 kg from 40 liters of feed) can be used as a good organic fertilizer.

Ultrafiltration

Transient Flux Decline

Flux decline behaviors of the effluent in turbulent and laminar flow regime are represented in Figs. 2 and 3, respectively. These figures illustrate that the time required to reach steady state decreases with an increase in the Reynolds number. Figure 2 shows that the steady state is attained in about 203 s, for Re = 4762 and 759 kPa pressure, whereas at Re = 5442 and Re = 6122, the steady states are attained within 172 s and 159 s, respectively at the same transmembrane pressure difference. As shown in Fig. 2, the flux decline is about 19% of the initial value for Re = 4762, about 16% with for Re = 5442, and 15% for Re = 6122. As the Reynolds number increases, the growth of the polarized layer over the membrane surface decreases due to enhanced forced convection and the steady state reaches at an earlier time. The resistance to the solvent flux also decreases with increase of cross flow velocity and permeate flux increases. Hence, the flux decline is lower at higher cross flow velocities. On the other hand, steady state is attained faster with an increase in operating pressure at a fixed cross flow velocity. For example, in Fig. 2, for Re = 4762, steady states are attained in about 166 s and 138 s respectively for 828 and 897 kPa pressures. Whereas at the same Re = 4762, time required to attain steady state is about 203 s for an operating pressure of 759 kPa. Steady state is achieved faster using a turbulent promoter compared to laminar flow. It

Table 3. Determination of optimum alum dose

Alum dose (wt%)	0.05	0.1	0.2	0.3	0.5	1	2	3	5
pH	11.46	11.2	10.86	10.15	9.74	7.75	6.8	4.7	4.25
TDS (g/l)	12.8	13.3	14.5	16.6	17.8	18.5	19	23.1	26.4
Conductivity $\times 10^{-1}$ (S/m)	20.1	20.5	22.2	23.8	25.4	27.0	28.7	33.1	37.7
TS (g/l)	50.7	50.5	50.3	50.0	48.8	48.1	47.2	48.9	50.6
COD (mg/l)	6720	6400	6080	5600	5120	4200	3500	3220	2940
Turbidity (NTU)	302	285	231	190	163	135	127	142	159

Table 4. Fertilizer quality of sludge

Sample	Sludge from liming	Vermi-compost
pH	7.3	7.1–7.8
Organic Carbon (wt%)	10.35	9.97–10.62
Nitrogen (wt%)	1.24	1.80
Phosphorous (wt%)	0.098	0.90
Potassium (wt %)	0.35	0.40

can be observed from Fig. 3 that at Re = 680 and 276 kPa, the steady state is attained in about 945 s without the promoter and about 785 s with the promoter at the same operating condition. The flux decline is about 38% without promoter at Re = 680 and 276 kPa pressure; but only 32% using promoter at the same operating condition. Turbulent promoters generate local turbulence and hence reduce the concentration polarization at the membrane surface. Steady state is established faster than without promoter as the growth of the polarized layer is controlled quickly. Therefore, the flux decline is also lower compared to the purely laminar condition.

Steady State

Figure 4 shows the variations of the steady state permeate flux with pressure at different Reynolds number under turbulent flow, and laminar flow without and

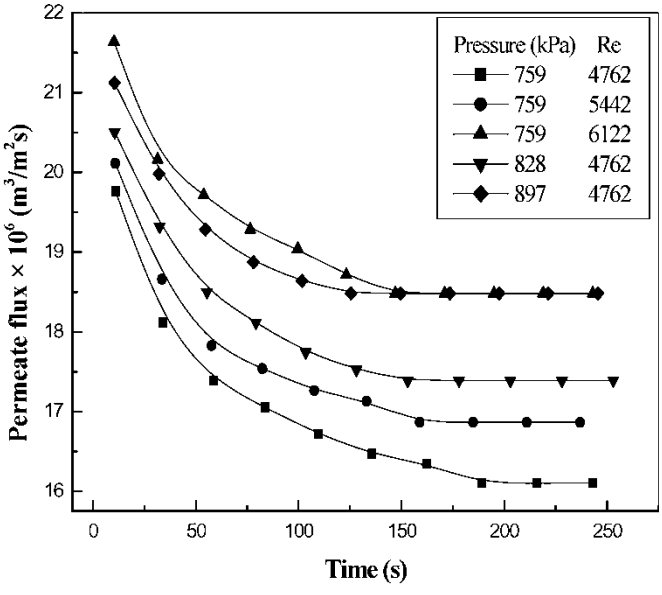

Figure 2. Transient flux decline of Turbulent flow regime in UF.

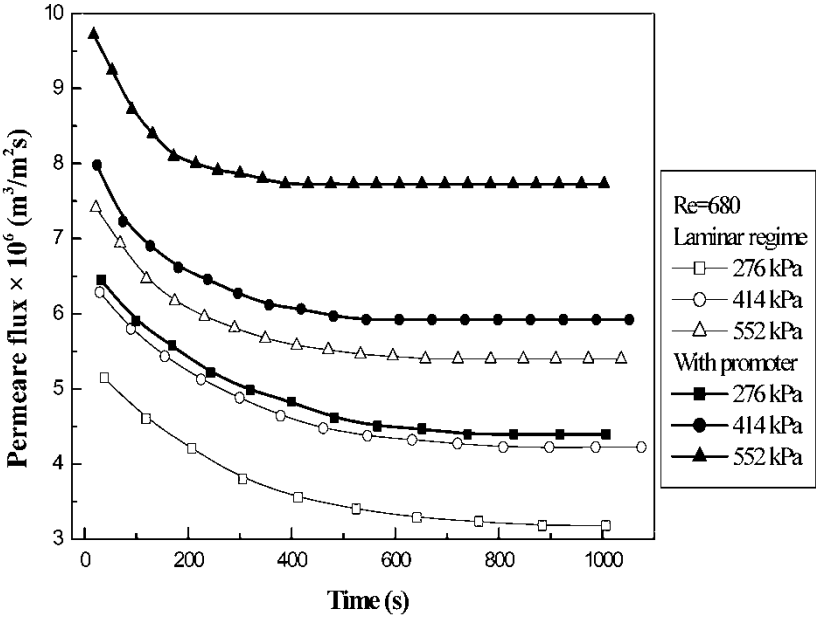

Figure 3. Transient flux decline of Laminar flow regime in UF.

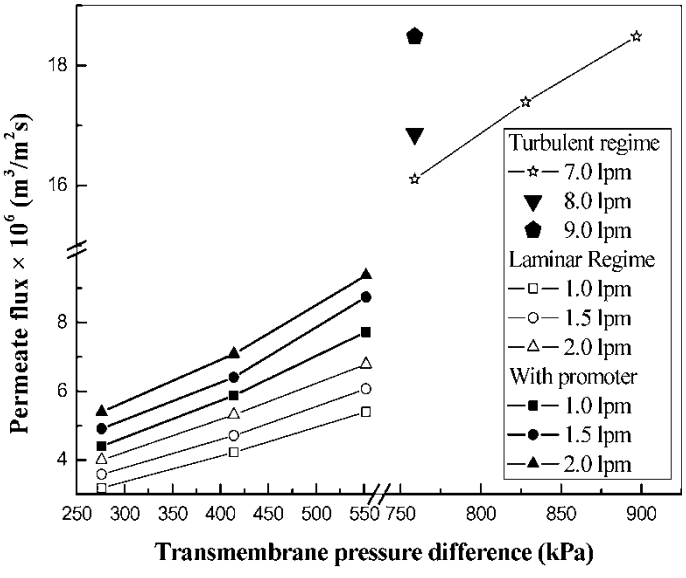

Figure 4. Variation of permeate flux with transmembrane pressure difference in UF.

with turbulent promoters. The figure shows that the flux increases with pressure and flow rate (Reynolds number), as expected. Higher flux is achieved at higher pressure due to increase in driving force. The increase in flux with flow rate (Reynolds number) is due to reduction in concentration polarization as discussed earlier. Figure 5 summarizes the percentage enhancements of the permeate flux in laminar regime with turbulent promoters for all the operating conditions. Flux enhancement is calculated taking the laminar flow results under the same operating conditions as the basis. It is observed from this figure that 35 to 44% flux enhancement is achieved under various operating conditions.

Analysis of Polarized Layer Resistance

The polarized layer resistance at the steady state is calculated as,

$$R_p^s = \frac{\Delta P}{\mu V_w^s} - R_m \tag{5}$$

for various operating conditions. For all hydrodynamic conditions, the variation of non-dimensional steady state polarized layer resistance with Reynolds number is represented in Fig. 6. The figure shows that the steady state values of R_p decrease with the Reynolds number as expected. For example, for a transmembrane pressure difference of 276 kPa in laminar flow, the ratio of the polarized layer and hydraulic resistance reduces from

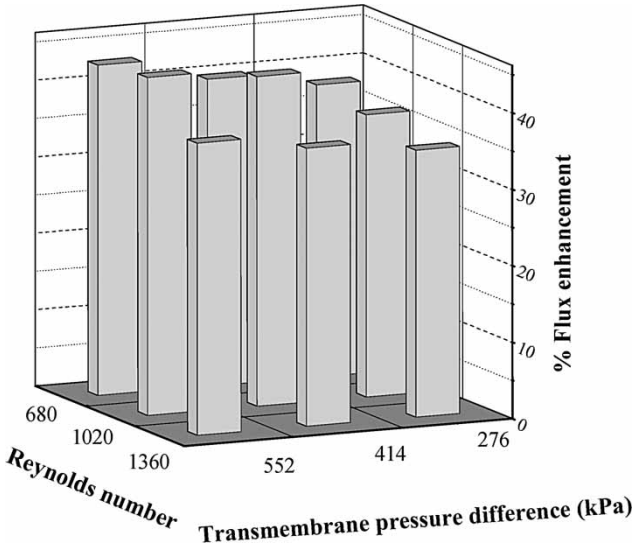

Figure 5. Flux enhancement with cross flow velocity and pressure in laminar regime with promoter in UF.

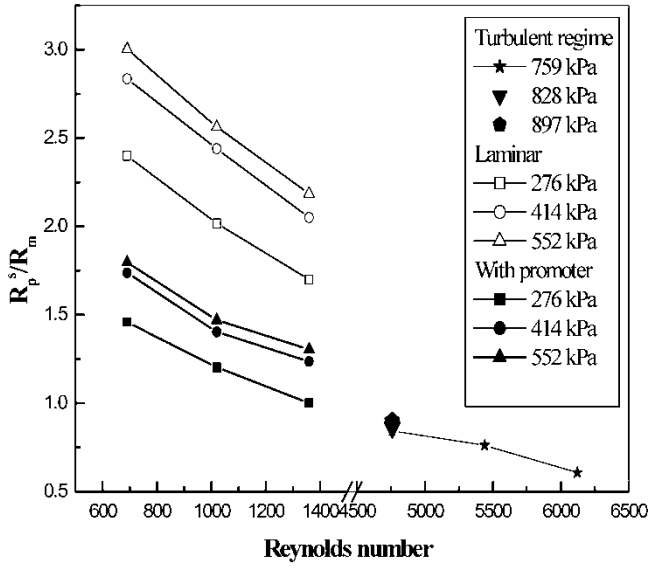

Figure 6. Variation of the ratio of polarized layer and hydraulic resistances at steady state with Reynolds number during UF.

2.4 to 2.0 with an increase in the Reynolds number from 680 to 1020. R_p values increase with the transmembrane pressure difference. With increase in pressure, more solutes are convected towards the membrane and this enhances the concentration polarization, resulting in increase in R_p values. For the case with the promoters, the polarized layer resistance decreases significantly due to the enhanced forced convection near the membrane surface induced by the promoters. At the same Reynolds number 680 and transmembrane pressure difference (276 kPa), the presence of turbulent promoters reduces the resistance to 1.5 compared to 2.4 in laminar flow. This reduction in R_p^s is more than 42% in some of the experiments leading to a significant enhancement of the permeate flux. The figure also shows further reductions in R_p at steady state for the case of purely turbulent flows for reasons already discussed. The steady state polarized layer resistance is correlated with the operating pressure and Reynolds number as,

$$\frac{R_p^s}{R_m} = a\left(\frac{\Delta P}{\Delta P_{\max}}\right)^{n1} (\mathrm{Re})^{n2} \tag{6}$$

where $\Delta P_{\max}$ is the maximum transmembrane pressure difference (897 kPa for UF and 1104 kPa for NF experiments). The values of lna, n_1, n_2 are presented in Table 5 for different hydrodynamic conditions. From equation (5), the steady state polarized layer resistance is calculated using the experimental

Table 5. Model constants

Operating condition	*lna*	n_1	n_2	r^2
Ultrafiltration				
Turbulent	10.67 ± 0.65	0.23 ± 0.004	-1.27 ± 0.006	0.96
Laminar	4.19 ± 0.32	0.35 ± 0.004	-0.47 ± 0.007	0.98
Laminar with promoter	3.86 ± 0.31	0.33 ± 0.004	-0.50 ± 0.007	0.98
Nanofiltration				
Turbulent	15.30 ± 0.82	0.23 ± 0.0036	-1.78 ± 0.006	0.98
Laminar	3.80 ± 0.11	0.42 ± 0.004	-0.39 ± 0.008	0.90
Laminar with promoter	4.23 ± 0.27	0.81 ± 0.0036	-0.51 ± 0.008	0.97

data at steady state for various operating conditions (operating pressure and cross flow velocity, i.e., the Reynold's number). Thereafter, the steady state polarized layer resistance is correlated with the operating conditions according to equation (6) using multiple regression analysis. The positive values of n_1 and negative values of n_2 confirm the trend of polarized layer resistance with the operating conditions as discussed earlier. It may be observed from Fig. 6 that the Reynolds number has a significant effect on the polarized layer resistance. For laminar flow with and without promoter, the polarized layer resistance is the major contributing resistance. For example, in case of pure laminar flow, at Reynolds number equal to 680 and transmembrane pressure difference at 276 kPa, R_m and R_p constitute about 29% and 71% of the total resistance, respectively. In case of laminar flow with promoter, at the same operating condition, contribution of R_p decreases significantly to 59% of the total resistance. For the turbulent flow regime, polarized layer resistances are generally less than the magnitude of the membrane hydraulic resistance. For the range of Reynolds number (Re = 4762 to 6122) studied herein, R_p^s varies between 0.6 to 0.9 times of R_m. At Reynolds number = 4762, R_p contributes about 46% of total resistance, whereas, at Reynolds number = 5442, it is about 43%.

The values of R_p^s at different operating conditions are evaluated from correlation presented in Eq. (6). Now, with these R_p^s values and experimentally observed R_p values, ln $(R_p^s/(R_p^s - R_p))$ is plotted at various time points for a fixed set of operating conditions, resulting into almost a straight line through the origin. The slope of these curves estimates the value of 'k' which is the kinetic rate constant of the growth of the polarized layer resistance. For laminar flow without promoter, the range of 'k' is 0.005 s^{-1} to 0.01 s^{-1}; for laminar flow with promoter, it is from 0.005 s^{-1} to 0.018 s^{-1} and for turbulent flow it is from 0.023 s^{-1} to 0.042 s^{-1}. Therefore, average values of 'k' are taken for calculating the profile of polarized layer resistance. The average value of 'k' is 0.0072 s^{-1} for laminar flow, 0.011 s^{-1} for laminar flow with promoter, and 0.031 for turbulent flow. Using the average 'k' values and equation (6) for R_p^s, the profiles of R_p are calculated and are

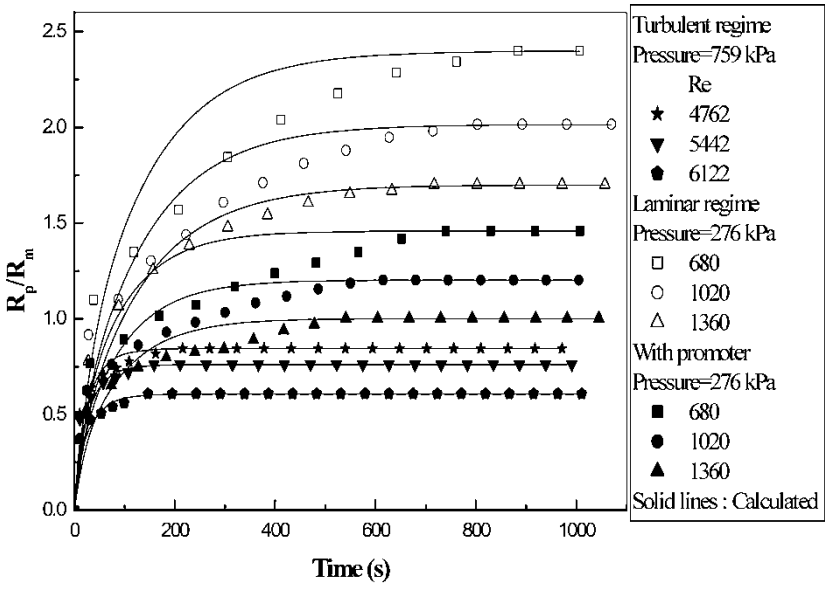

Figure 7. Variation of calculated dimensionless polarized layer resistance with time in UF.

presented in Fig. 7 for various operating conditions. It is observed from Fig. 7 that the calculated profiles of R_p match closely with the experimental values specially for long time of operation. At earlier period of filtration, the matching is somewhat moderate. This may be due to experimental errors involved in measurement of earlier flux values. It is also possible that the initial rate follows a different rate equation than used in this study. Moreover the quality of fit increases appreciably if individual 'k' values are used instead of an average 'k' as was done here. Further work is needed to explain the behavior completely. For all the hydrodynamic conditions, the R_p values are lower at higher Reynolds number as expected.

Permeate Quality

Figure 8 represents the variation of COD with transmembrane pressure difference at the operating Reynolds number (turbulent, laminar, and with turbulent promoter). With an increase in transmembrane pressure difference the permeate quality in terms of COD decreases and with Reynolds number, the permeate quality improves. With increase in pressure, the solvent flux as well as solute flux increase linearly and thus COD of the permeate increases. As the Reynolds number increases, the growth of the polarized layer over the membrane surface is reduced due to enhanced forced convection as discussed earlier. So the solute concentration of the permeate

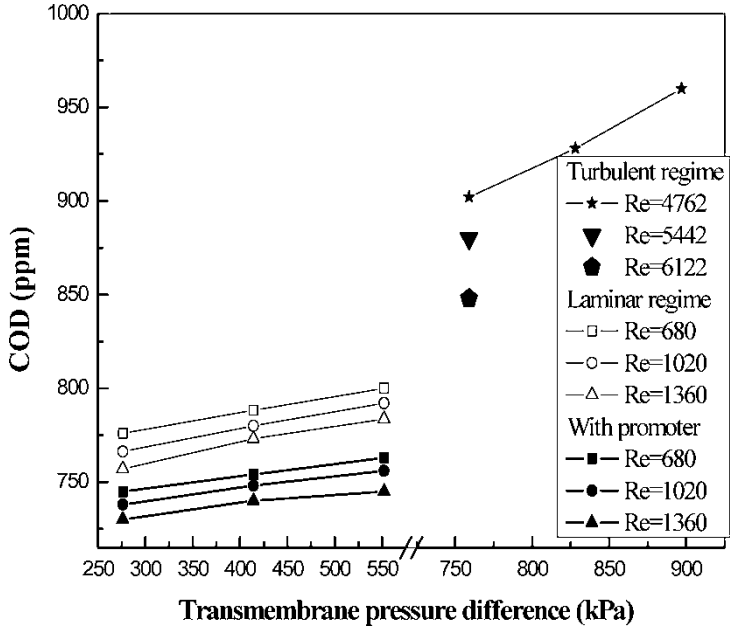

Figure 8. Variation of COD with transmembrane pressure difference in UF.

decreases and as a result of which COD decreases. It can also be observed from Fig. 8 that at 276 kPa pressure and Re = 680, COD is 776 where as at 552 kPa pressure and at same Re, the COD is 800. It is also observed that at 552 kPa pressure and Re = 680, COD decreases by about 5% in the presence of promoter compared to laminar at the same operating conditions. At Re = 4762, as the transmembrane pressure difference increases from 759 kPa to 897 kPa, COD increases by 6%. For a transmembrane pressure difference of 759 kPa, COD reduces from 902 to 848 with an increase in the Reynolds number from 4762 to 6122. Since all the salt present in the feed solution has permeated through the UF membrane, the permeate conductivity remains almost the same as that of the feed.

Nanofiltration

Around 10 l UF permeate is collected for NF treatment in turbulent, laminar and laminar with turbulent promoters at different operating conditions (Table 2).

Transient Flux Decline

As in the case of UF, the time needed to reach steady state decreases with increase in cross flow velocity and transmembrane pressure difference and

also in the presence of turbulent promoters. The extent of flux decline also follows similar trends for reasons already discussed in the section titled Transient Flux Decline. At 828 kPa pressure the flux decline is about 32% of the initial value at a Re = 680 and is 25% at the same operating conditions but with promoters. About 828 s is required to reach steady state with promoter whereas about 1071 s is needed without promoter in laminar regime at 828 kPa pressure.

Steady State Flux

Figure 9 shows the variation of steady state permeate flux with Reynolds number and transmembrane pressure difference in NF. The figure clearly shows that as in the case of UF the permeate flux increases with operating pressure and the Reynolds number. About a 24% increase in permeate flux is observed at 1104 kPa and an increase in the Reynolds number from 4762 to 6122. The flux enhancement is about 41% for the laminar flow with promoter at Re = 1020 at 966 kPa pressure taking the laminar flow results under the same operating conditions as the basis. The permeate flux enhancement varies from 27% to 47% for various operating conditions.

Analysis of Polarized Layer Resistance

The variation of non-dimensional steady state polarized layer resistance with transmembrane pressure difference, for all the hydrodynamic conditions, is

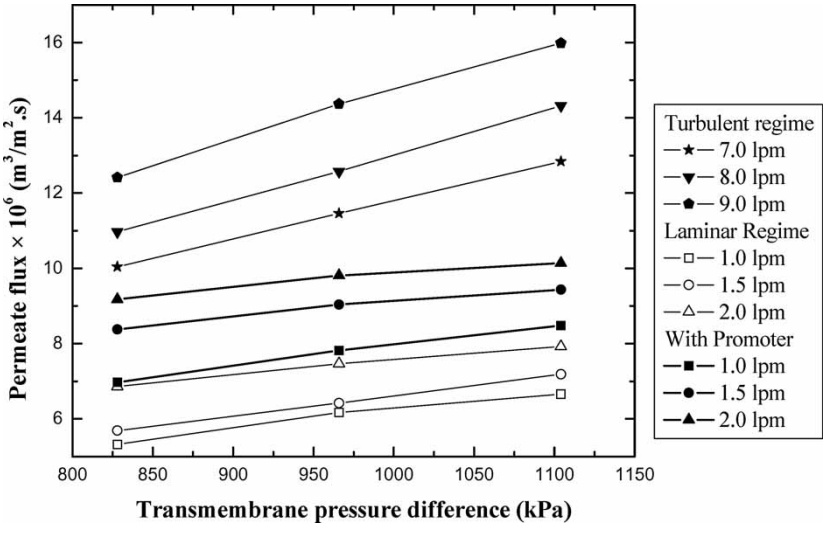

Figure 9. Variation of permeate flux with transmembrane pressure difference in NF.

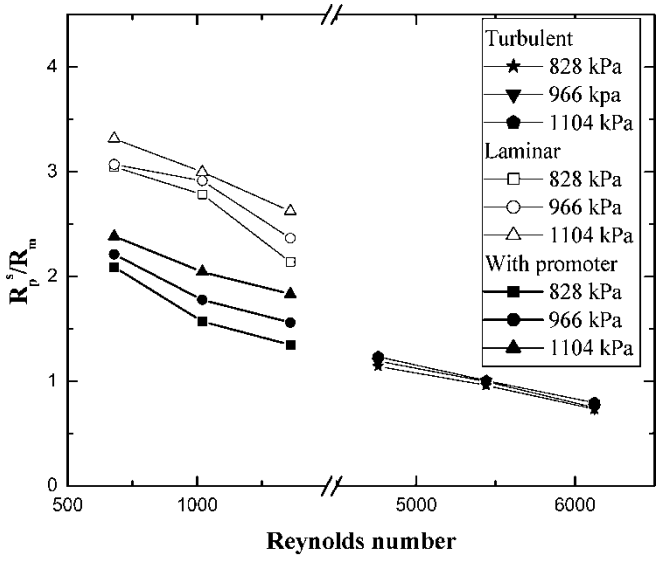

Figure 10. Variation of the ratio of polarized layer and hydraulic resistances at steady state with transmembrane pressure difference in NF.

represented in Fig. 10. The steady state values of R_p increase marginally with the transmembrane pressure difference and decrease significantly with an increase in the Reynolds number as discussed earlier. For example, the dimensionless polarized layer resistance increases from 2.8 to 3.0 when pressure increases from 828 to 1104 kPa, at Re = 1020. Increase in polarized layer resistances is marginal with pressure for laminar flow with promoter and for all cases of turbulent Reynolds numbers. This clearly indicates that the polarized layer is almost incompressible within the pressure range studied here. The presence of turbulent promoters reduces the polarized layer resistance. For example, at 828 kPa pressure polarized layer resistance decreases by about 31%, when promoters are introduced. Under turbulent flow conditions, the effect of the Reynolds number is more striking on the polarized layer resistance. For example, for all the operating pressure values, polarized layer resistance varies from 0.7 to 1.2, which are significantly less compared to those under laminar flow conditions (2.1 to 3.3) and under laminar flow with promoter (1.3 to 2.4). At 828 kPa pressure, R_p/R_m value decreases by about 36% when the Reynolds number increases from 4762 to 6122. Under turbulent conditions, the polarized layer resistance becomes comparable to the membrane hydraulic resistance. At 828 kPa pressure, it contributes about 48% to the total resistance. Contribution of polarized layer resistance is about 62% with promoter and is about 72% without promoter (under laminar flow condition) at the same operating pressure level.

For turbulent flow regime, the R_p^s/R_m values are fitted with the operating conditions as given in equation (6) and the estimated parameters are tabulated in Table 5. For the growth of R_p/R_m, 'k' values are fitted using equation (5). Average 'k' values are found to be 0.007 s^{-1} for laminar flow, 0.009 s^{-1} for laminar flow with promoter, and 0.02 s^{-1} for turbulent flow. The calculated and experimental R_p values are presented in Fig. 11 for all operating conditions. Figure 11 shows a close match between the calculated and experimental data, except the data during the early operation. This may be due to errors involved in the measurement of flux data during the initial period of experiments. It is also possible that the initial rate follows a different rate equation than used in this study. Moreover the quality of fit increases appreciably if individual 'k' values are used instead of an average 'k' as was done here. Further work is needed to explain the behavior completely.

Permeate Quality

Variations of permeate COD with trans-membrane pressure at the operating Reynolds number in turbulent, laminar, and with turbulent promoter are shown in Fig. 12. It is observed that with the increase in transmembrane pressure difference and the Reynolds number, the permeate quality improves. With increase in pressure, the solvent flux increases linearly, while the solute flux is nearly independent of pressure for less open membranes (RO and in some cases for NF membranes) (16). This indicates that with increasing pressure, more solvent passes through the membrane along with a fixed amount of the solute; the permeate becomes purer and

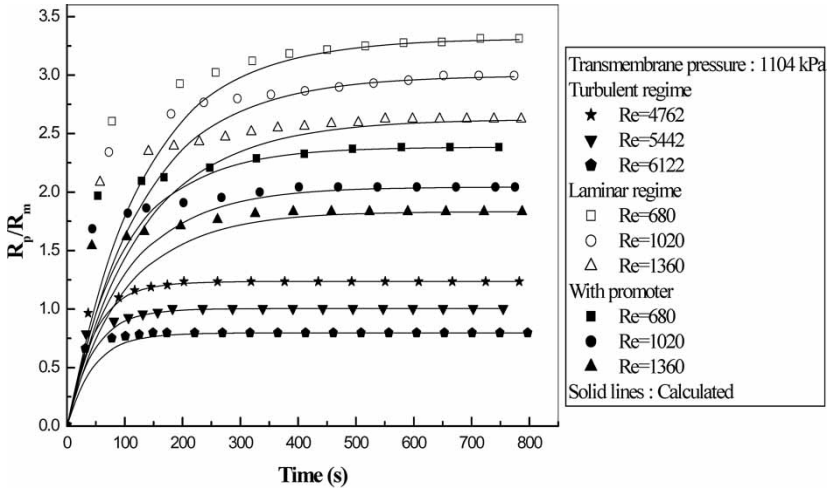

Figure 11. Variation of calculated dimensionless polarized layer resistance with time in NF.

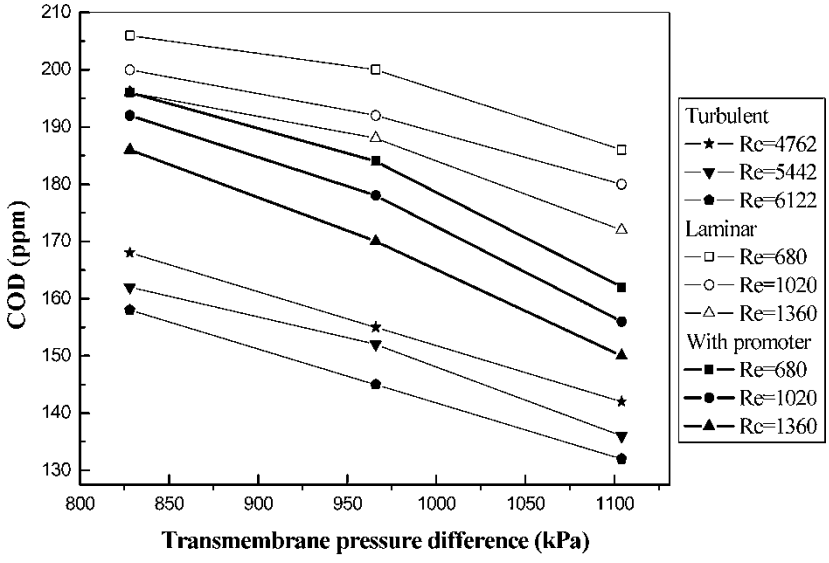

Figure 12. Variation of COD with transmembrane pressure difference in NF.

hence the permeate quality (expressed as COD) increases. Similar trends are observed for laminar flow with promoter and turbulent flow. It can be seen from Fig. 12 that at 828 kPa pressure and Re = 1360, COD decreases by about 11% in the presence of promoter compared to the base case (laminar at same operating conditions). Percentage decrease in COD is found to be about 13% at 966 kPa pressure and Re = 1360 and also about 13% at 1104 kPa pressure and Re = 1360. At Re = 4762, as the transmembrane pressure difference increases from 828 kPa to 1104 kPa, COD decreases by 15%. From the figure it may also be observed that COD in the permeate varies from about 206 to 132 ppm in the pressure range of 828 to 1104 kPa which is much lower than the permissible limit (250 ppm). Table 6 shows other properties for various operating conditions in NF. Permeate conductivity is the same as the feed which indicates that almost all the salt present in the feed solution has permeated through the NF membrane.

CONCLUSION

The viability of liming unit effluent treatment using a combined process of coagulation by alum and membrane separation is established in this study. The values of COD ($\sim$164 ppm) of NF are well below the discharge limit. With increase in the Reynolds number and applied pressure the time required to reach the steady state decreases. Permeate flux enhancements using turbulent promoters in laminar regime (35–44% for UF and 27–47% for NF) are observed. Polarization resistance is the major contributor to

Table 6. Permeate analysis after nanofiltration

Sr. No	Reynolds number	Pressure kPa	TDS ppm	TS ppm	pH	Conductivity $\times 10^{-1}$ (S/m)	Ca^{++} ppm	CI^{-} ppm
Turbulent regime								
1	4762	828	11800	20500	7.4	17.9	1090	18020
2	5442	828	11700	20400	7.39	17.3	1080	18000
3	6122	828	11600	20300	7.4	17.4	1090	18100
4	4762	966	11800	21300	7.44	17.9	1100	18060
5	5442	966	11400	21300	7.4	17.4	1080	18100
6	6122	966	11300	21000	7.37	17.1	1090	18040
7	4762	1104	11600	20800	7.41	17.3	1090	18000
8	5442	1104	11600	20600	7.4	17.6	1080	18020
9	6122	1104	11500	20200	7.4	17.4	1070	18040
Laminar regime								
1	680	828	12000	25600	7.35	18	1080	18100

2	1020	828	11900	25300	7.34	18.1	1060	18020
3	1360	828	11800	25000	7.35	17.9	1070	18080
4	680	966	11800	24800	7.4	17.9	1090	18060
5	1020	966	11800	24700	7.41	17.8	1080	18100
6	1360	966	11700	24500	7.39	17.8	1040	17980
7	680	1104	11800	24000	7.35	17.8	1070	18040
8	1020	1104	11800	23600	7.42	17.8	1090	18000
9	1360	1104	11800	23000	7.42	17.8	1070	18020
With Turbulent Promoter								
1	680	828	11800	23500	7.41	17.4	1060	17960
2	1020	828	11700	23200	7.4	17.9	1040	17960
3	1360	828	11600	23000	7.41	17.4	1050	18020
4	680	966	11700	22600	7.39	17.8	1040	17980
5	1020	966	11600	22500	7.42	17.2	1040	18020
6	1360	966	11500	22500	7.41	17.9	1050	18010
7	680	1104	11500	22100	7.41	17.4	1070	18100
8	1020	1104	11700	22000	7.42	17.8	1040	18000
9	1360	828	11800	21800	7.44	17.8	1060	17940

overall resistance, both in UF and NF, to the solvent flow for laminar and laminar with promoter case. However, for turbulent flow conditions, the polarized layer resistances are 0.8 to 0.9 times the membrane hydraulic resistance for UF and 0.7 to 1.2 times for NF. A first order kinetic model suitably describes the growth rate of polarized layer resistance. Pulverized sludge obtained after sun drying can be used as organic fertilizer.

NOMENCLATURE

v_w	permeate flux ($m^3/m^2 \cdot s$)
v_w^s	steady state permeate flux ($m^3/m^2 \cdot s$)
ΔP	transmembrane pressure difference (kPa)
ΔP_{max}	maximum transmembrane pressure difference (kPa)
R_m	membrane hydraulic resistance (m^{-1})
R_p	polarized layer resistance (m^{-1})
R_p^s	steady state polarized layer resistance (m^{-1})
k	kinetic rate constant of the growth of polarized layer resistance (s^{-1})
t	time (s)
μ	viscosity ($Pa \cdot s$)
Re	Reynolds number
a, n_1, n_2	model constants (Equation (6))

ACKNOWLEDGEMENTS

This work is partially supported by a grant from the Department of Science and Technology, New Delhi, Government of India under scheme no. DST/TSG/WM/2005/55. Any opinions, findings, and conclusions expressed in this paper are those of the authors and do not necessarily reflect the views of DST.

REFERENCES

1. Espantaleón, A.G., Nieto, J.A., Fernández, M., and Marsal, A. (2003) Use of activated clays in the removal of dyes and surfactants from tannery waste waters. *Appl. Clay Sci.*, 24: 105–110.
2. Raghava Rao, J., Chandrababu, N.K., Muralidharan, C., Nair, B.U., Rao, P.G., and Ramasami, T. (2003) Recouping the wastewater: a way forward for cleaner leather processing. *J. Cleaner Prodn.*, 11: 591–599.
3. Ahmed, M.T., Taha, S., Chaabane, T., BenFarès, N., Brahimi, A., Maachi, R., and Dorange, G. (2005) Treatment of sulfides in tannery baths by nanofiltration. *Desalination*, 185: 269–274.

4. Vidal, G., Nieto, J., Cooman, K., Gajardo, M., and Bornhardt, C. (2004) Unhairing effluents treated by an activated sludge system. *J. Hazard. Materials*, B112: 143–149.
5. Suthantharajan, R., Ravindranath, E., Chitra, K., Umamaheswari, B., Ramesh, T., and Rajamani, S. (2004) Membrane application for recovery and reuse of water from treated tannery wastewater. *Desalination*, 164: 151–156.
6. Chakraborty, S., Purkait, M.K., DasGupta, S., De, S., and Basu, J.K. (2003) Nanofiltration of textile plant effluent for color removal and reduction in COD. *Sep. Purif. Technol.*, 31: 141–151.
7. Afonso, M.D. and Pinho, M.N.D. (1991) Membrane separation processes in pulp and paper industry. *Desalination*, 85 (1): 53–58.
8. Jönsson, A.S. and Trägårdh, G. (1990) Ultrafiltration applications. *Desalination*, 77: 135–179.
9. Ball, P. (2000) Scale-up and scale-down of membrane-based separation processes. *Membr. Technol.*, 117: 10–13.
10. Baker, R.W. (1991) Membrane separation systems-recent development, future direction. Noyes Data Corporation, 329.
11. Cassano, A., Molinari, R., Romano, M., and Drioli, E. (2001) Treatment of aqueous effluents of the leather industry by membrane processes A review. *J. Memb. Sci.*, 181: 111–126.
12. Das, C., DasGupta, S., and De, S. Treatment of soaking effluent from tannery using membrane separation processes. Accepted to *Desalination*.
13. Cassano, A., Drioli, E., and Molinari, R. (1998) Integration of ultrafiltration into unhairing and degreasing operations. *J. Soc. Leather Technologists Chemists*, 82: 130–135.
14. Das, C., Patel, P., De, S., and DasGupta, S. (2006) Treatment of tanning effluent using nanofiltration followed by reverse osmosis. *Sep. Purif. Technol.*, 50: 291–299.
15. Trivedy, R.K. and Goel, P.K. (1986) *Chemical and Biological Methods for Water Pollution Studies*; Environmental Publications: Karad.
16. Bungay, P.M., Lonsdale, H.K., and Pinho, M.N.D. (1983) *Synthetic Membranes: Science, Engineering and Application*; D. Reidel Publishing Company.